Regular three-dimensional bubble clusters: shape, packing and growth-rate

S.J. Cox[1]*and **F. Graner**[2] †

[1] Department of Pure and Applied Physics, Trinity College, Dublin 2, Ireland.

[2] Laboratoire de Spectrométrie Physique, Boîte Postale 87, F-38402 St. Martin d'Hères Cedex, France.

Abstract

We consider three-dimensional clusters of identical bubbles packed around a central bubble and calculate their energy and optimal shape. We obtain the surface area and bubble pressures to improve on existing growth laws for three-dimensional bubble clusters. We discuss the possible number of bubbles that can be packed around a central one: the "kissing problem", here adapted to deformable objects.

Pacs numbers: 82.70.Rr, 83.80.Iz

1 Introduction

1.1 Motivation

Bubbles, such as soap bubbles, are objects with simple geometry and physical properties. But when two or more bubbles cluster together, how well do we really understand their properties?

The limiting case of a cluster of many bubbles, known as a foam, is usually approached with continuum approximations. An understanding of foam properties such as aging, due to gas diffusion, and structure is a problem of fundamental interest stimulated by the need to predict the

---

*Corresponding author: Tel:+353 1 6083165; Fax +353 1 6711759; Email: simon.cox@tcd.ie

†CNRS UMR 5588 & Université Grenoble I

behaviour of foam in industrial applications. From carbonated drinks to the processes used to extract gold ore from the earth, foams are an important part of our lives with various industrial uses [1, 2].

The alternative to the continuum description, described here, is an approach based upon the study of finite clusters of bubbles. Its advantage is the ease with which we can obtain precise structural information. This has been demonstrated convincingly in two-dimensions (2D), where exact results exist for two problems of paramount interest:

- The Kelvin problem: what is the least energy (equivalent to line-length) structure of equal-size bubbles that fills space? In 2D, Hales [3] proved that this is the familiar honeycomb structure. In 3D, where the problem is one of minimizing surface energy or area, no such exact result exists. Kelvin [4] gave a candidate structure, still believed to be the best for a structure containing *identical* cells, although in the general case it has since been beaten by the Weaire-Phelan structure [5] consisting of bubbles of two different types. The important quantity in this problem is the surface area of each face of a bubble of unit volume, or equivalently the normalized total surface area $S/V^{2/3}$.

- Growth laws: how does a foam age, or *coarsen*, due to gas diffusion across its surfaces? The 2D result, due to [6], says that the growth-rate of a bubble (of area A) is directly linked to its number of sides, n: $dA/dt \propto (n-6)$. That is, it depends upon bubble topology only, irrespective of the precise geometry. In 3D, the growth law is written [7]:

$$\frac{\mathrm{d}V^{2/3}}{\mathrm{d}t} = \frac{1}{2}\Sigma_i \frac{\Delta p_i S_i}{V^{1/3}} \tag{1}$$

where the sum is taken over each face, which has a pressure difference Δp_i and area S_i. Again, the normalized area appears to be important, but does the 3D growth law depend only on the bubble topology? In fact it does not, but it may make sense to express the average growth-rate of F-faced bubbles as a function of F only *if* the dispersion about such a law is small.

1.2 State of the art

The study of 3D foam coarsening was pioneered by Glazier [7], who used a 3D Potts model to numerically simulate foam coarsening. He proposed a linear growth law $\Sigma_i \Delta p_i S_i \propto (F - cst)$ for bubbles with a number of faces F from 6 to 57 (and even from 4 to 60, with some numerical uncertainty). Similar linear laws were observed in subsequent experiments involving optical tomography and reconstruction using the Surface Evolver [8] (F between 9 and 16), and magnetic resonance imaging experiments [9, 10] for F from 4 to 26.

This growth law was refined by three detailed results presented by Hilgenfeldt et al. [11]: first, an approximate analytical formula based upon regular F-faced polyhedra with curved faces:

$$\frac{\mathrm{d}}{\mathrm{d}t} V^{2/3} = G(F) = \frac{3}{2^{1/3}} \left[(F-2) \tan \left(\frac{\pi}{\eta_F} \right) \right]^{2/3} \tan^{1/3} \left(\frac{\chi_F}{2} \right) \left(\frac{\pi}{3} - \chi_F \right) \tag{2}$$

where $\chi_F = 2 \tan^{-1} \sqrt{4 \sin^2(\pi/\eta_F) - 1}$ and $\eta_F = 6 - 12/F$ is the number of edges per face. Second, a (non-explicit) correction for non-regular faces; third, numerical (Surface Evolver) simulations for foams containing bubbles with F from 5 to 42. Recently, Cox and Fortes [12] also used the Surface Evolver to calculate numerically the structural properties of single "regular" bubbles with surfaces of constant mean curvature; this gave information for certain values of F between 2 and 32.

1.3 Outline of this paper

Here, we study clusters consisting of one bubble surrounded by F others, each with prescribed volumes. This constitutes a finite cluster with free boundary conditions: this represents a realistic foam surrounded by air, in contrast to the idealized bubbles described by Hilgenfeldt et al. [11]. We chose such an approach, which neglects long-distance correlations between bubbles, because it should provide more physical insight than existing experiments and simulations, and enable more precise calculations than the analytical approach. Within this "mean-field" choice, all results presented below are exact, without approximations. Moreover, in principle we should have access to all physically realizable values of F.

In the course of our study of the equal-volume case, we encountered what we call "the kissing

problem for (deformable) bubbles". Our simulations allow us to ask: how many deformable (dry) bubbles can be packed around one other? The original kissing problem, discussed by Gregory and Newton, was: how many identical hard spheres can surround one other, each touching the central one [13]? In two-dimensions the answer is obvious and well-known – only six hard discs can be packed around one other, in the familiar honeycomb arrangement. For the three-dimensional problem, consideration of the angle subtended by each sphere at the central one suggested that the maximum number could be as high as 14, but Newton was correct in believing that only 12 neighbours are possible [14]. We will show that for bubbles these critical numbers are 12 (2D) and 32 (3D).

The plan of the paper is as follows. We first describe our method of cluster preparation and relaxation. There are limits, for each set of given bubble volumes, to the values of F for which stable clusters exists. In the equal-volume case we offer a solution to the kissing problem. We then analyse in more detail the shape and growth-rate of many different bubbles, and present predictions about coarsening and quantify the spread of the growth-rate about the growth law (2).

2   Definitions and methods

We take a central bubble of volume V_c and surround it with F bubbles, each with the same volume V; this is the natural extension into 3D of the 2D "flower" of [15]. To create and equilibrate such a cluster, we use a Voronoi construction with VCS [16] and then the Surface Evolver [17], as follows.

We must first make a choice about the topology of the cluster. Since we wish to create the cluster using a Voronoi routine, we must first choose an arrangement of $F + 1$ points about which to create bubbles.

We first place a point at the origin of a sphere of radius 1. Then the Voronoi points are placed at the positions given by the solution of the "covering radius problem" [13]: the arrangement of F points on the unit sphere that minimizes the maximum distance of any point from its closest neighbour. Candidates to the solution of this problem have been given by [18] for F from 4 to 130, which is exactly what is required for our purpose. Note that this is not the only way to pack the F Voronoi points, but appears (partly with hindsight) to have been a good choice – it gives all the
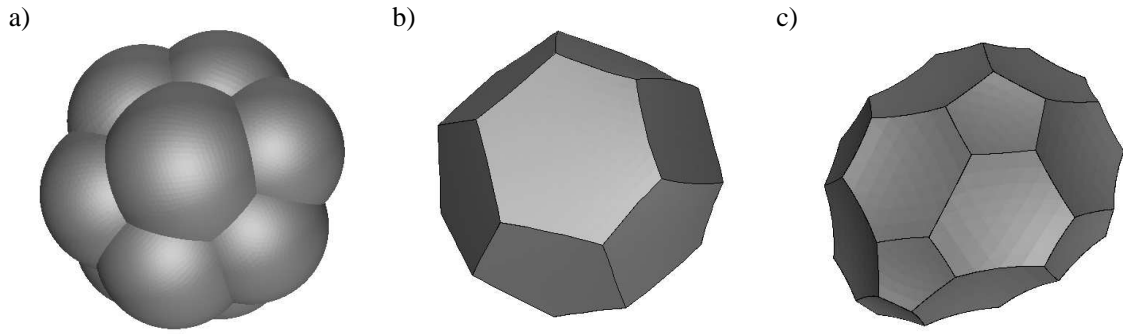
Figure 1: Examples of the clusters considered here with $V_c = V = 1$ in each case: (a) cluster of $F = 13$ "petals" (that is, a total of $F + 1 = 14$ bubbles) still attached; (b) the central bubble, drawn to a different scale, with $F = 13$ faces (one square, ten pentagons and two hexagons); (c) a bubble with $F = 26$ faces (all pentagonal or hexagonal) – note its departure from approximate sphericity, described in §3.2.

arrangements we know to expect, e.g. for $F = 6, 12, 32$.

We truncate the Voronoi diagram by adding $3F$ points at a radial distance of 2 from the origin. We ensure that these outer points are at least a distance $2\varepsilon/\sqrt{3F}$ apart, decreasing ε from 1 until a solution is found, usually at around $\varepsilon = 0.8$. This data is put through the VCS software; the output file is then transferred to the Surface Evolver, version 2.18d. We use two levels of refinement and quadratic mode, to obtain a high level of accuracy.

We compute the following quantities for the ith face ($i = 1, \cdots, F$) of the central bubble: its number of sides n_i, area S_i and pressure difference Δp_i. Then for the whole bubble we record its volume V, its normalized total line length $L/V^{1/3}$, its normalized surface area $S/V^{2/3}$ (where $S = \Sigma_i S_i$), and its growth-rate through eq. (1), which we plot as a function of F.

3 Topology and limits for equal-volume clusters

We first consider the case where the volume of the central bubble is equal to that of its neighbours, $V_c = V$. Examples of such monodisperse clusters are shown in figure 1 for $F = 13$ and 26. This illustrates that despite the rather symmetric initial condition (putting points on a sphere) we can still obtain significantly skewed bubbles after relaxation.
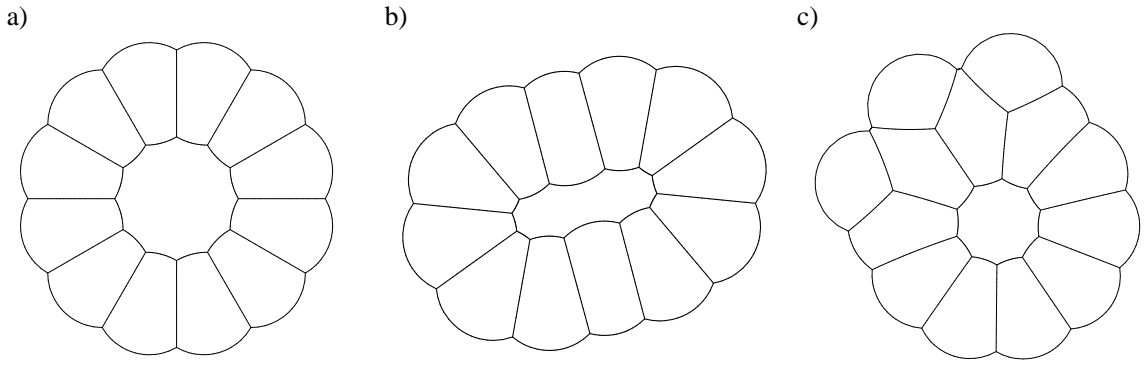
5

Figure 2: (a) A symmetrical 2D flower cluster with $F = 12$ petals and $A_c/A = 2$. (b) One of the possible stable buckled states of the same cluster with $A_c = A$. (c) One of the possible "ejected" states [20] with $F = 13$ petals and $A_c = A$.

3.1 The kissing problem for 2D bubbles

For completeness, we consider first the two-dimensional problem. How many 2D bubbles can be packed around one other of the same area?

Our initial pattern is that of the "flower" clusters introduced recently [15, 19, 20]. It consists of a central cell of area A_c surrounded by F identical petals of area A. A symmetric example with $F = 12$ petals and $A_c = 2A = 2$ is shown in figure 2(a). A priori, one could imagine that the number of petals could increase without limit, with the F sides of the central bubble becoming increasingly curved.

However, Weaire et al. [15] showed that for $F > 6$ there is a "buckling" instability at a critical ratio of the bubble areas given approximately by

$$A_c/A \approx 0.04(F - 6)^2.$$

For unit areas and $F > 6 + (0.04)^{-1/2} = 11$, the symmetric shape is therefore no longer stable, the flower becomes "floppy" and many modes of buckling, corresponding to different shaped central bubbles, are possible (all with the same energy). An example for $F = 12$, in which there is an elliptical mode of buckling, is shown in figure 2(b).

Is it possible to pack even more bubbles? We find that for $F > 12$, any of the buckled configurations of clusters with unit areas are unstable to a topological change caused by the length of one of the internal edges shrinking to zero [20]. An example is shown in figure 2(c) for $F = 13$, for

which three bubbles are "ejected" in an equilibrium configuration with $A_c/A = 1$.

Thus we conjecture that the maximum number of bubbles that can touch the central one is 12. This is twice the value for hard discs.

3.2 The kissing problem for 3D bubbles

In three dimensions the idea is the same. In principle one could imagine that there should be no limit to the number of bubbles which will fit around the central one, albeit with the latter being hugely distorted. However, since the area of each of the five-sided faces shrinks as F increases, our simulations of bubbles with unit volumes, $V_c/V = 1$ do not find a stable cluster for all possible numbers of petals. In fact, we could only find clusters for $5 \leq F \leq 32$. That is, we cannot obtain a bubble with more than 32 faces and volume equal to that of its neighbours which satisfies Plateau's laws after energy (surface area) minimization.

For most values of F, the shrinkage of five-sided faces is accelerated by an ellipsoidal distortion of the central bubble (see figure 1(c)), due to the asymmetric location of the pentagonal faces amongst the hexagonal ones. Might there be a discontinuous buckling transition for 3D clusters? As a result of further simulations, we believe not: this asymmetry, and the consequent elliptical deformation of the central bubble, means that the transition to the asymmetric pattern is continuous.

It is interesting to note that the case $F = 32$ is special: it is probably the most symmetric cluster for $F > 12$ – it corresponds to the C_{60} Buckminster fullerene. Hence, by analogy, one might expect that stable clusters with unit volumes exist for higher order carbon structures. We tried C_{80} ($F = 42$) and the elliptical C_{72} ($F = 40$) and didn't find them to be stable. We thus conjecture that no more than 32 bubbles can touch the central one: 32 appears to be the "kissing" number for 3D bubbles. Recall that for hard spheres the kissing number is 12.

4 Shape, pressure and growth-rate

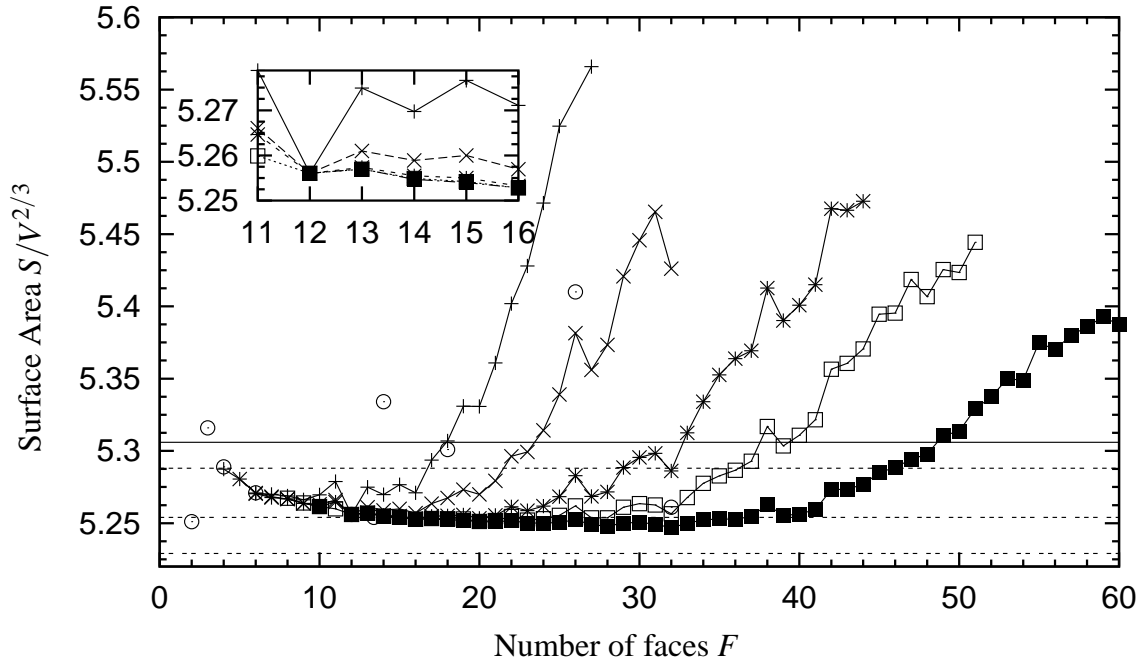We next analyse in detail the statistics of the bubbles found in our simulations.

Figure 3: The normalized surface area $S/V^{2/3}$ varies, albeit over a small range, non-monotonically as F increases. Inset: zoom over the range $F = 11$ to 16. Data is shown for volume ratios of $V_c/V = \frac{1}{2}(+), 1(\times), 2(\ast), 3(\square)$ and $5(\blacksquare)$. For all values of the volume ratio V_c/V, the pentagonal dodecahedron at $F = 12$ has the same value of $S/V^{2/3}$, but for all other F the surface area fluctuates widely, although in general it decreases as the volume ratio increases. Also shown is the data for bubbles with constant curvature ($\odot$) rather than with fixed volume [12]. Shown as horizontal lines (from top to bottom) are the value of $S/V^{2/3}$ for the Kelvin structure (solid line), for the Weaire-Phelan structure (quadruple dashes), for the "ideal" bubble (triple dashes) and for an infinitely large bubble with hexagonal faces (double dashes) [21].

4.1 Equal-volume bubble clusters

We consider first the monodisperse case, relevant to the Kelvin problem, where the volume of the central bubble is equal to that of its neighbours, $V_c = V$. As mentioned above, we can go from F = 5 to 32. The ratio $S/V^{2/3}$, shown in figure 3, is lowest at $F = 12$, and increases steeply for F greater than about 16.

The inset on figure 3 shows the data around the optimal region $F = 11$ to 16. These bubbles, which do not pack to fill space, have lower area than Kelvin's (5.306) and even Weaire-Phelan's (5.288) (see [22] for details of other space-filling foam structures). They are barely above the value
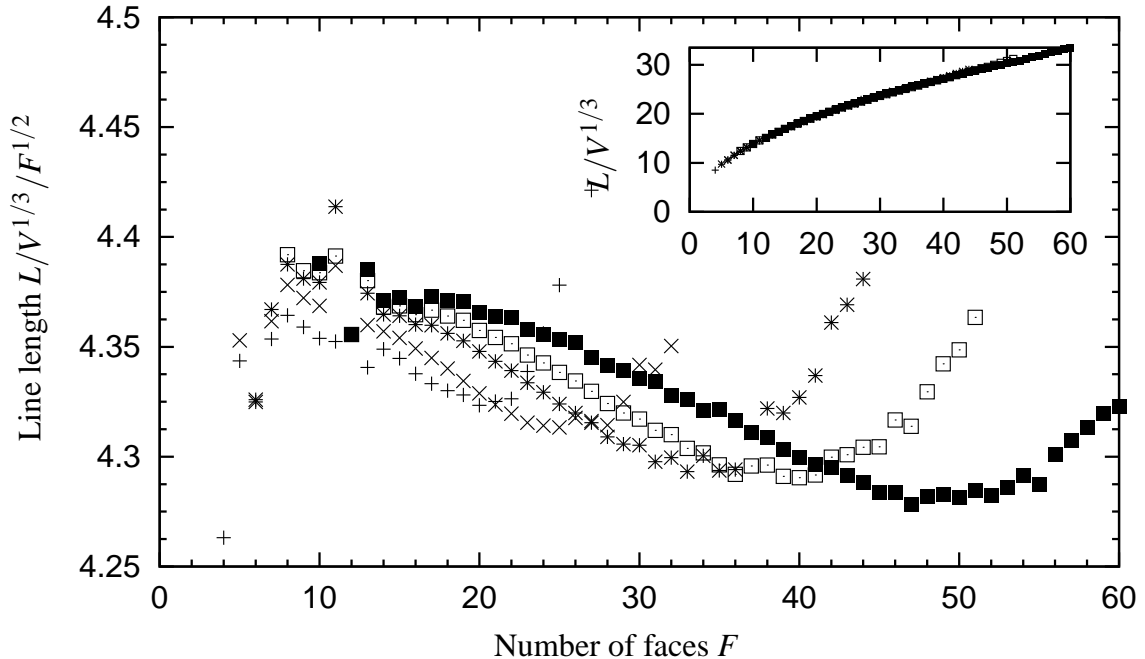
Figure 4: The line-length ratio $L/V^{1/3}$ increases in proportion to the square-root of F [12] (inset). We therefore plot the ratio $L/V^{1/3}/F^{1/2}$, for volume ratios of $V_c/V = \frac{1}{2}(+), 1(\times), 2(*), 3(\square)$ and $5(\blacksquare)$. The data is everywhere close to $L = 4.35V^{1/3}F^{1/2}$, confirming the square-root behaviour. The dispersity increases as both F and V_c/V increase.

for the so-called "ideal" bubble (5.254) [23]. The latter, with $F = 13.39$, describes a regular (but unphysical) "bubble" which would have flat faces, and hence a growth-rate of zero.

Also of interest is the normalized line-length $L/V^{1/3}$ of each bubble, plotted in figure 4. Note that all data lies close to a line $L/V^{1/3} \propto \sqrt{F}$ [12]. We therefore show the ratio $L/V^{1/3}/F^{1/2}$ in figure 4: the maximum deviation (i.e. the shallow minimum in the data) occurs for $F \approx 25$.

4.2 Non-equal volumes

4.2.1 Simple volume ratios

We next consider the case where the volume of the central bubble is not equal to the volume of its neighbours. There are again limits to the possible stable clusters, but they vary with the volume ratio. We study the simple ratios $V_c/V = \frac{1}{2}, 2, 3$ and 5. This choice of volume ratios allows us to explore F from 4 to 60.

Note that the possible range of F is not always continuous. For instance, we cannot construct

9

a stable cluster with 26 neighbours for $V_c/V = \frac{1}{2}$, hence we find $F \in [4-25, 27]$. Similarly, 11 neighbours is unstable for $V_c/V = 5$, and we find $F \in [10, 12-60]$.

For each value of F we record the topology of each bubble, collated for all volume ratios (table 1), using the notation n_x to mean that the bubble has x-faces with n-sides. The topology of the central bubble might depend on V_c/V: we find such non-uniqueness in only two instances. We accept this as due to the slight randomness used in placing the $3F$ outer points to truncate the initial Voronoi pattern.

The line-length, shown in figure 4, fall close to the same curve as in the monodisperse case. The square-root approximation becomes slightly worse as the bubbles become larger and gain more faces, with the maximum deviation occurring at higher F for increasing V_c/V.

4.2.2   Large volume ratios

With larger V_c/V we can look at bubbles with many faces and very low surface areas. For instance, with $F = 122$ (corresponding to the fullerene C_{240}) and $V_c/V = 200$ we find a bubble with topology $5_{12}6_{110}$ and $S/V^{2/3} = 5.239$: see figure 5.

We could extend this process to larger bubbles with more faces. The normalized area should eventually approach the value for an infinitely large bubble with hexagonal faces: $S/V^{2/3} = 5.229$ [21]; note that this is not the theoretical lower bound for the normalized area, which corresponds to a spherical bubble with $F - 1$ infinitesimally small neighbours [24].

4.2.3   Correlations

Real foams often have a distribution of bubble volumes, and their topology is correlated to the geometry: larger bubbles tend to have more neighbours [25].

Such correlations appear in our results, although we did not specifically include them. Their physical origin is clear. In fact, consider a bubble of volume V_c, and consider the average of its neighbours' volumes, denoted V (mean-field description). Then, for this given V_c/V ratio, the physically realizable values of F are limited. Within the possible F, the $S(F)$ curves admit an optimum: there is a value of F which minimizes the bubble area. These optimal F values do increase with V_c/V. Moreover, on figure 3 we can read the optimal surface $S_{\text{opt}}/V^{2/3}$ as a function

10

Table 1: The topology of each central bubble, where n_x denotes the number x of n-sided faces.

* denotes configurations for $F = 2$ and 3 from [12].

** denotes alternative configurations for given F with different V_c/V: $F = 11$ ($4_2 5_8 6_1$ for $V_c/V = 3$) and 34 ($5_{14} 6_{20}$ for $V_c/V = 2$).

| F	Topology	F	Topology	F	Topology	F	Topology
1	–	16	$5_{12} 6_4$	31	$5_{13} 6_{17} 7_1$	46	$5_{12} 6_{34}$
2	$1_2{}^*$	17	$5_{12} 6_5$	32	$5_{12} 6_{20}$	47	$5_{14} 6_{31} 7_2$
3	$2_3{}^*$	18	$5_{12} 6_6$	33	$5_{13} 6_{19} 7_1$	48	$5_{12} 6_{36}$
4	3_4	19	$5_{12} 6_7$	34	$5_{12} 6_{22}{}^{**}$	49	$5_{12} 6_{37}$
5	$3_2 4_3$	20	$5_{12} 6_8$	35	$5_{14} 6_{19} 7_2$	50	$5_{12} 6_{38}$
6	4_6	21	$5_{12} 6_9$	36	$5_{14} 6_{20} 7_2$	51	$5_{12} 6_{39}$
7	$4_5 5_2$	22	$5_{12} 6_{10}$	37	$5_{12} 6_{25}$	52	$5_{13} 6_{38} 7_1$
8	$4_4 4_4$	23	$5_{12} 6_{11}$	38	$5_{12} 6_{26}$	53	$5_{13} 6_{39} 7_1$
9	$4_3 5_6$	24	$5_{12} 6_{12}$	39	$5_{12} 6_{27}$	54	$5_{12} 6_{42}$
10	$4_2 5_8$	25	$5_{12} 6_{13}$	40	$5_{12} 6_{28}$	55	$5_{14} 6_{39} 7_2$
11	$4_3 5_6 6_2{}^{**}$	26	$5_{12} 6_{14}$	41	$5_{12} 6_{29}$	56	$5_{12} 6_{44}$
12	5_{12}	27	$5_{12} 6_{15}$	42	$5_{12} 6_{30}$	57	$5_{12} 6_{45}$
13	$4_1 5_{10} 6_2$	28	$5_{12} 6_{16}$	43	$5_{12} 6_{31}$	58	$5_{12} 6_{46}$
14	$5_{12} 6_2$	29	$5_{12} 6_{17}$	44	$5_{12} 6_{32}$	59	$5_{12} 6_{47}$
15	$5_{12} 6_3$	30	$5_{12} 6_{18}$	45	$5_{13} 6_{31} 7_1$	60	$5_{12} 6_{48}$
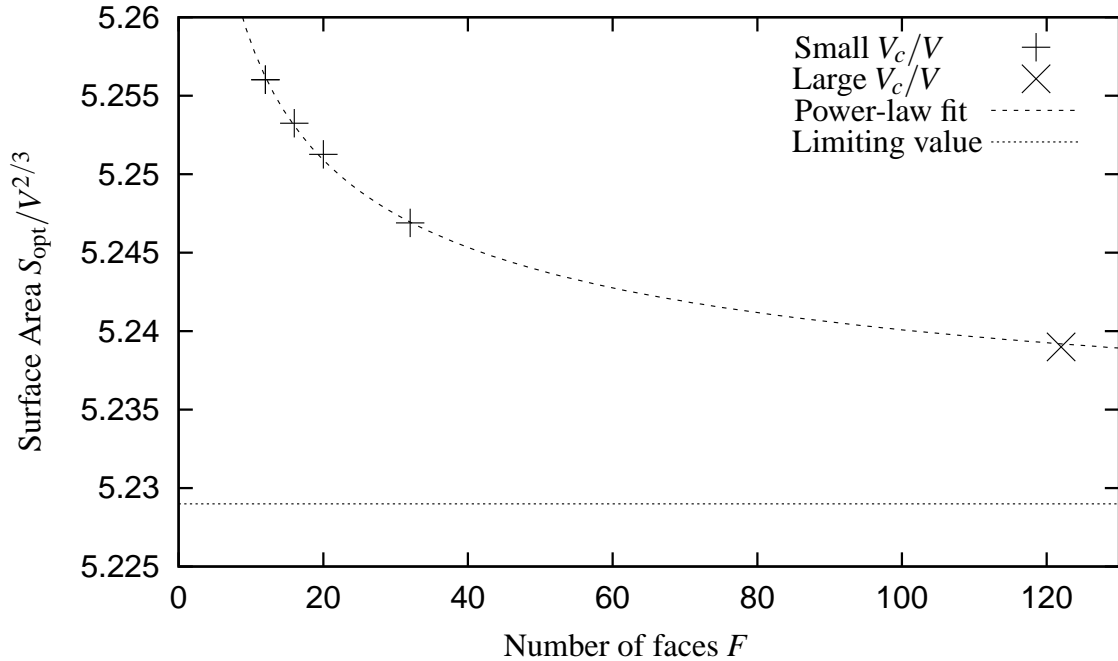
Figure 5: The optimal normalized surface area $S_{\rm opt}/V^{2/3}$ for a range of values of the volume ratio V_c/V. Data are shown for values of $V_c/V = 1, 2, 3$ and 5 (+) and for the representative calculation for $F = 122$ with $V_c/V = 200$ (×). The limiting value for $V_c/V \to \infty$ at $S/V^{2/3} = 5.229$ is shown as a horizontal line and we also show a power-law fit: $S/V^{2/3} = 5.229 + 0.078/F^{0.423}$.

of F: it is the envelope of all curves plotted, shown in figure 5. It decreases roughly as one over the square-root of F as the volume ratio increases.

In 2D, the expression for $L_{\rm opt}/A^{1/2}$ *versus n* has been used to estimate the energy of a 2D foam [26], then to determine the correlations between geometry (area *A*) and topology (number of sides *n*) [27]. Here, its 3D counterpart, the $S_{\rm opt}/V^{2/3}$ *versus F* relation, is more complicated (in particular, unlike in 2D, it depends on the volume ratio): but it appears to have the same essential property as in 2D, namely to be a non-increasing function of *F*; we thus hope to extend to 3D this 2D result [27].

4.3 Growth-rate

As a result of these simulations, we are able to calculate the instantaneous growth-rate of many bubbles, with many different numbers of sides, through the formula (1). It is shown in the inset to figure 6 – all data lies close to (2), except at (for us unobtainable) small *F* where the results of Cox

Table 2: The growth-rates, averaged over all simulations, for bubbles with few faces, $F < 12$. They differ significantly from the analytic equation (2) [11], but show very little dispersion.

F	2	3	4	5	6	7	8	9	10	11
$-\mathrm{d}V^{2/3}/\mathrm{d}t$	5.632	4.655	3.967	3.326	2.849	2.350	1.899	1.506	1.130	0.760

and Fortes [12] are useful.

More instructive is the difference between the analytic formula and our data, shown in figure 6. For $F \geq 12$, our data are above and below the analytic line: it agrees with the suggestion that the analytic formula approximates the average growth-rate [11], and quantifies the dispersion around this average (less than 1 % dispersion). Conversely, for $F < 12$, our data are clustered and significantly (up to 10 %) larger than the analytical formula, which confirms that the analytical approximations gradually lose their validity at low F, as expected [11]. In a coarsening foam, the bubbles with low F are important because it is these bubbles that disappear. So although for $F \geq 12$ the growth-rate is well approximated by (2), we give in table 2 the growth-rates for bubbles with $F < 12$, averaged over all simulations.

5 Conclusions

Using the Surface Evolver, we have studied finite clusters of bubbles to give information about the structure of three-dimensional foam and a 3D coarsening law. This approach allows us to get a high level of detail and accuracy of the relevant quantities (surface area, pressure difference) to get a good insight into how foams evolve. Our calculated values of the growth law require no assumption about the curvature being small, and can be found for bubbles with an arbitrary number of faces.

As the volume ratio between the central bubble and its neighbours changes, we find upper and lower bounds on the possible number of faces, because the bubbles deform. This leads us to conjecture a value for the kissing problem for foams: no more than 32 bubbles can be stably packed around one other of the same volume.
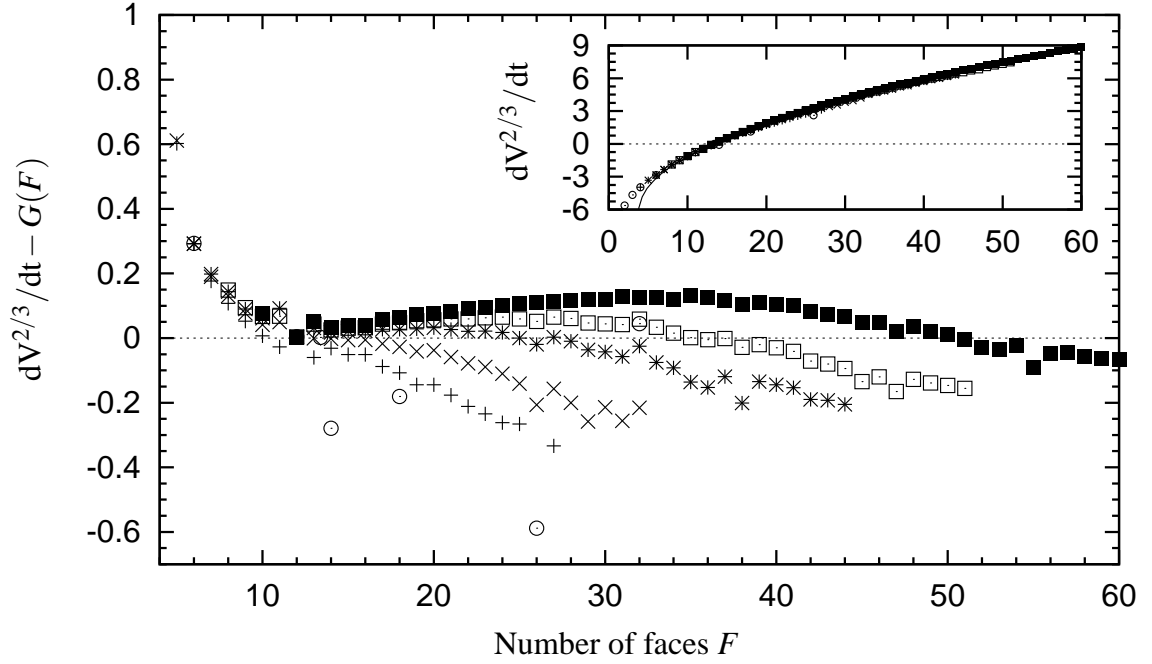
Figure 6: The difference in the rate of change of volume of a bubble with F faces, calculated from our simulations using (1), and the value calculated according to the analytic formula (2). The inset shows the values themselves, again next to the analytic line, from which it deviates at small F. Data is shown for volume ratios of $V_c/V = \frac{1}{2}(+), 1(\times), 2(\ast), 3(\boxdot)$ and $5(\blacksquare)$. The data for bubbles with constant curvature ($\odot$) [12], rather than fixed volume, is more scattered, but useful for low F.

Although we don't tackle infinite (or, equivalently, periodic) structures, we expect that this data will eventually lead to greater insight into the Kelvin problem, since we are starting to understand better what happens for bubbles with between 12 and 16 faces.

Acknowledgements

References

[1] D. Weaire and S. Hutzler. (1999) *The Physics of Foams*. Clarendon Press, Oxford.

[2] P. Zitha, J. Banhart and G. Verbist (eds). (2000) *Foams, emulsions and their applications*. MIT-Verlag, Bremen.

[3] T.C. Hales. (2001) *Discrete Comput. Geom* **25**:1.

[4] W. Thomson. (1887) *Phil. Mag.* **24**:503.

[5] D. Weaire and R. Phelan. (1994) *Phil. Mag. Letts.* **69**:107.

[6] J. vonNeumann (1952) In *Metal Interfaces* pp. 108. American Society for Metals, Cleveland.

[7] J.A. Glazier. (1993) *Phys. Rev. Lett.* **70**:2170.

[8] C. Monnereau and M. Vignes-Adler. (1998) *Phys. Rev. Lett.* **80**:5228.

[9] C.P. Gonatas, J.S. Leigh, A.G. Yodh, J.A. Glazier and B. Prause. (1995) *Phys. Rev. Lett.* **75**: 573.

[10] J.A. Glazier and B. Prause (2000) In P. Zitha, J. Banhart and G. Verbist (ed), *Foams, Emulsions and their applications*. MIT-Verlag, Bremen pp. 120.

[11] S. Hilgenfeldt, A.M. Kraynik, S.A. Koehler and H.A. Stone. (2001) *Phys. Rev. Letts.* **86**: 2685.

[12] S.J. Cox and M.A. Fortes. (2003) *Phil. Mag. Letts* **83**:281.

[13] J.H. Conway and N.J.A. Sloane. (1999) *Sphere Packing, Lattices and Groups*. Springer, New York.

[14] J. Leech. (1956) *Math. Gaz.* **Feb**:22.

[15] D. Weaire, S.J. Cox and F. Graner. (2002) *Eur. Phys. J. E* **7**:123.

[16] J. Sullivan. (1988) `http://torus.math.uiuc.edu/jms/software/`.

[17] K. Brakke. (1992) *Exp. Math.* **1**:141.

[18] R.H. Hardin, N.J.A. Sloane and W.D. Smith. (1994) Coverings by points on a sphere `http://www.research.att.com/~njas/coverings/`.

[19] K.A. Brakke and F. Morgan. (2002) *Euro. Phys. J. E* **9**:453.

[20] S.J. Cox, M.F. Vaz and D. Weaire. (2003) *Eur. Phys. J. E* **11**:29.

[21] S. Hilgenfeldt, A.M. Kraynik, D.A. Reinelt and J.M. Sullivan. (2003) In preparation.

[22] A.M. Kraynik, D.A. Reinelt and F. van Swol. (2003) *Phys. Rev. E* **67**:031403.

[23] C. Isenberg. (1992) *The Science of Soap Films and Soap Bubbles*. Dover, New York.

[24] K. Brakke. (2002) Private Communication.

[25] D. Weaire and J.A. Glazier. (1993) *Phil. Mag. Lett.* **68**:363.

[26] F. Graner, Y. Jiang, E. Janiaud and C. Flament. (2001) *Phys. Rev. E* **63**:011402.

[27] M.A. Fortes and P.I.C. Teixeira. (2003) *J. Phys. A: Math. Gen.* **36**:5161.